Developing laminar flow in the inlet length of a smooth pipe

S.A. AL-NASSRI and T. UNNY*

Visiting Professor, Civil Engineering, University of Waterloo, Canada; and Vice-President, University of Technology, Baghdad, Iraq.
*Professor, Civil Engineering, University of Waterloo, Ontario, Canada.

Abstract. The laminar flow phenomena in the inlet (entrance) region of circular pipe are investigated experimentally. New curves of friction factor versus Reynolds number, for various entry lengths, are obtained and compared with the standard curve for fully developed laminar flow. The relationship between the viscous friction, the energy loss due to the lengthwise rate of change of the kinetic energy coefficient and the total energy loss is investigated. The continuous variation of the velocity profile is analysed by using the concept of a non-Newtonian liquid whose shear sensitivity varies continuously along the pipe.

Nomenclature

A	cross-sectional area
α	kinetic energy correction coefficient
D	pipe diameter
δ	boundary thickness
Δ	increment
f	measured friction factor as defined by Darcy's law
f_k	component of f due to change in kinetic energy only
f_v	component of f due to viscous head loss only
f_L	friction factor as computed from Langhaar's theory
g	gravitational acceleration
h	head loss
H_k	component of h due to change in kinetic energy
H_v	component of h due to viscous friction
K, n	constants in the power law $\tau = K(\mathrm{d}U/\mathrm{d}r)^n$
v	kinematic viscosity
μ	viscosity
L	length
L_e	entry length
L_d	developing (inlet) length
N_R	Reynolds number
P	pressure
Q	volume discharge
r	distance from the centre line of the pipe towards the wall
r_0	radius
ρ	pressure
τ	shear stress

Applied Scientific Research 36: 313–332 (1981) 0003–6994/81/0365–0313 $03.00.

U velocity
U_m mean velocity
U_c centre-line (maximum) velocity
x_1 axial distance from entrance to the first pressure tapping point
x_2 axial distance from entrance to the second pressure tapping point
Z dimensionless number $= L/r_0$
ξ dimensionless number $= Z/N_R$

Introduction

The study of Newtonian fluid flow in the entrance region of a pipe is of considerable interest and is of practical application in, for instance, a short pipe leading to a diffuser or nozzle. Figure 1 is a diagrammatic sketch of developing flow in a pipe.

The total inlet (entrance) length, pressure gradient and velocity profile developments along the inlet length have been the interest and concern of many engineers and scientists over the years. The problem is somewhat difficult and of a sensitive nature. To simplify the problem some assumptions are usually made by the investigators, and the accuracy of the solution will no doubt depend on these assumptions as well as on the method adopted. Schiller [7] was the first to investigate the lengthwise laminar flow development in smooth pipes. He used an integral approach of the velocity profile within the boundary layer; the pipe radius in the parabolically developed flow was replaced by the boundary thickness 'δ'. In this method the viscous dissipation in the boundary layer was neglected and hence resulted in some inaccuracy. Langhaar [5] simplified the problem by linearizing the inertia terms in the equation of motion. His approach resulted in an approximate solution and to some extent quantitave suspect as will be shown by the present investigation. Whittington and Ashton [12] carried out extensive experimental work on the development of flow in a 4.46 mm copper pipe with a bell-mouth entrance. The shift in the friction factor f versus Reynolds number N_R curve is consistent with Langhaar's theory but is greater than that

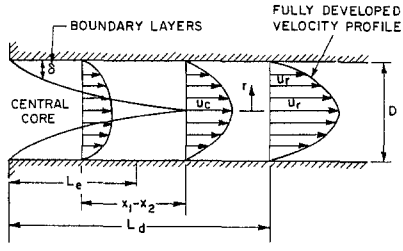

Figure 1. Diagrammatic sketch of developing flow in a pipe

predicted by his theory. To date, many researchers have developed various methods and approaches for an improved solution to the problem. Van Dyke [10] summarizes the methods which have been applied, also Fargie and Martin [3] and Vrentas and Duda [11] highlight the work of various investigators in this field such as Tatsumi [9], Collins and Schowalter [2], Campbell and Slattery [1], Friedmann et al. [4] and Schlichting [8].

The Fargie and Martin method based on the differential and integral momentum equations of flow is of noticeable simplicity and leads to a good approximate solution for laminar flow. Most recently, Mohanty and Asthana [6] used an interesting technique predicting a longer entrance length compared with that of previous investigators, to achieve the fully developed laminar flow as defined by Poiseuille's law. Their analysis is based on dividing the flow in the entrance length into two lengthwise regions: the inlet and the filled region. The former is the section between the entrance and the point where the boundary layers meet at the pipe axis, but the velocity profile beyond this section is not yet similar. The filled region starts at the end of the inlet region and extends to the point where Poiseuille's similar profile is attained. Thus, in the filled region, adjustment of the completely viscous profile takes place. Mohanty and Asthana's study is limited to laminar flow and has been verified experimentally for Reynolds number of 1875, 2500 and 3250 only.

Present investigations

From the preceding review it is clear that most of the work done so far deals with theoretical predictions, although in a few cases some experimental verification has been carried out for limited values of Reynolds number. Furthermore, to some extent discrepancies exist between the various results obtained. Measurements of flow development and associated changes in pressure gradient along the entrance length are somewhat sparse; this conclusion is also shared by Fargie and Martins [3].

The present investigation covers an extensive range of experiments in the inlet (entrance) length of smooth circular pipes. The experimental results are compared with the thoeretical ones predicted by other investigators. The continuous variation in the velocity profile along the inlet length is analysed by using the concept of a non-Newtonian liquid whose shear sensitivity varies continuously along the pipe. The functional relationship $f = \phi(N_R, L/D)$ along the inlet length is thoroughly defined and compared with the other available data.

In this paper the term 'inlet length (L_d)' refers to the distance from the entry which is 'long enough' for the flow to become stable (at constant Reynolds number) and beyond which the velocity profile does not change. Some texts refer to it as 'entrance length', 'development length' or 'transition length'. The actual distance from the entry to the point midway between the pressure-loss tappings will be called 'entry length' (L_e), which may thus be less than, equal to, or greater than the inlet length.

Experimental apparatus

The experiments were conducted in a closed circulation system, a diagram of which is shown in Figure 2. The water is supplied to the pipe under investigation from a tank of constant head, more than 27 m high. The pipe is screwed between entry and exit boxes, which provide a sharp entrance situation. The boxes are 12.8 m apart and are designed to house a circular pipe of 6.35 mm (1/4 in) in diameter and made of perspex. The discharge through the pipe is controlled by gate and needle valves. The quantity measurement was made with the weigh bridge for large discharges, and for small flows volumes were measured.

A horizontal steel channel beam, with pieces of wood to support the beams, was provided at every 1.2 m with grooved supports on top to receive the pipe. Each piece of wood had four foot screws so that the pipe could be levelled. A number of pressure taps were made along the pipe at suitable distances from the entry. A special technique was developed to ensure that the pressure was measured at the centre line of the pipe section. Figure 3 shows a typical tapping block made of perspex. The water from the pipe enters the block through four holes 1.6 mm (1/16 in) at right angles. The block is made of two pieces which can easily be mounted on the pipe. Three types of pressure gauges in the form of a U-tube manometer were used covering different ranges of flow.

Experimental procedure and measurements

Since this investigation was of a sensitive nature, considerable care had to be taken in all measurements for maximum accuracy. The exact diameter of the pipe was determined by filling a small cut from the tube with water and using

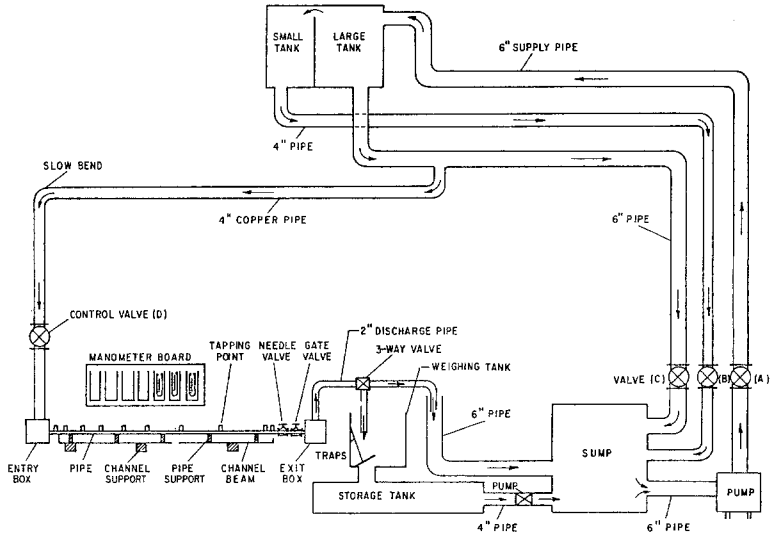

Figure 2. General arrangement of the apparatus (not to scale).

the weight-density relationship. A check was also made using a micrometer gauge and a steel rule. The variation was found to be ± 0.051 mm and the average inside diameter was equal to 6.35 mm. The mercury, dibromopentane liquid and paraffin manometers were calibrated for the temperature range expected.

In order to provide a constant head during the experiment, the pump was switched on all the time, with the supply valve (A), (Figure 2) sufficiently opened so that there was a continuous overflow from the large tank into the small tank. The valve (B) of the small tank was fully opened so that the overflow returned to the sump. The water to the pipeline was drawn from the large tank, which was full all the time.

Great care had to be taken in reading the manometers. First of all the air in the pipe and the manometer leads was carefully expelled, the zero reading for all the manometers in use being a good indication that all the air was expelled. The control valves at the end of the pipeline were then opened and each manometer was read when the flow head had become steady. The fluctuation in the manometer levels were reasonably small for all the test lengths except for those which were very close to the entrance. However, the flow became progressively less steady as the transition was approached. Fluctuations in the gauges became very considerable, especially for Reynolds

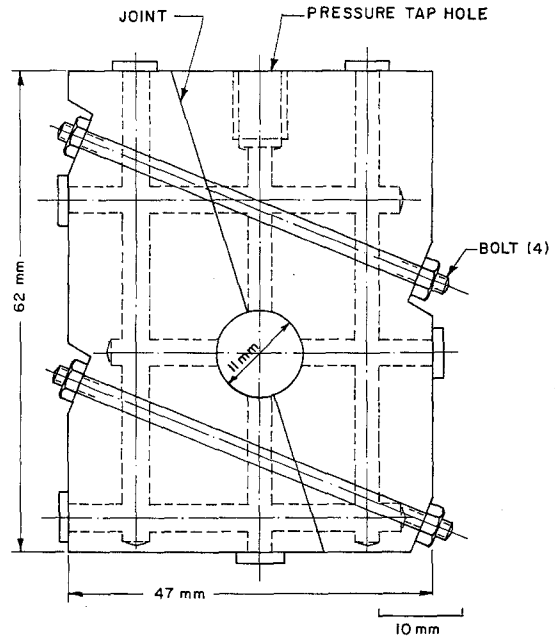

Figure 3. Detail of the pressure tapping block for the pipe

Table 1. Summary of the experimental tests

Test length 1st pressure tapping point	2nd pressure tapping point	Distance from entry (mm) 1st point	2nd point	Entry length/ diameter	No. of discharges considered
1	2	58	152	16.5	29
2	3	152	500	51.4	28
3	4	500	857	106.9	24
4	5	857	1215	163.2	24
6	7	1938	2656	361.7	35
8	9	4083	5518	756.0	37
9	10	5518	6153	919.0	25

numbers between 2000 and 3000. For this reason, in the transition zone, all measurements were repeated four or five times to ensure a satisfactory average. The discharge for each steady state was measured at least twice to eliminate any possible error. Also, a note was made of the water temperature for every run.

It was expected that the effect of entrance would decrease exponentially as the distance from the entrance increased. It therefore seemed logical to distribute the pressure-tapping points or 'stations' so that they were closest together in the regions of greatest interest, becoming more sparse as the entrance was left behind. Table 1 summarizes the test lengths considered and the corresponding entry lengths. The tapping points chosen provided a range of entry lengths between approximately 16 and 900 diameters. The range of Reynolds numbers considered was 324–15,478.

Figures 4–10 summarize the results in the form of a graph of the friction factor versus Reynolds number for the above seven test lengths. A computer program was written to plot the results on a large scale of 0.1 mm accuracy in order to obtain a clear picture of the variation in the curves. Langhaar results and the lengthwise fully developed flow equations are shown in each graph to enable comparisons to be made, as will be seen in the analysis and discussion of the results.

Friction factor in the inlet length – analytical treatment

The value of the friction factor 'f' in the inlet length 'L_d' may be considered to be due partly to the viscous friction and partly to the change in kinetic energy. If we denote the value of 'f' due to the former only by f_v and that due to the latter only by f_k, then a relationship between f, f_v and f_k must exist. In the experiments carried out the total (combined) coefficient of friction is measured. However, it is desirable to derive expressions for the values of f_v and f_k and their relationship. In this section a new approach to the variation of f_v and f_k with N_R and L_e/D is made.

An expression for f_v

Consider a concentric cylinder of liquid, (Figure 11). In the inlet length, the shear stress τ does not increase linearly as the distance r from the centre increases. The relationship may be expressed in the general form $\tau = K(dU/dr)^n$, where dU/dr is the velocity gradient across the diameter; n is a function of N_R and the entry length to diameter ratio L_e/D. The limits of n are 0 at the entry and 1 at the end of the inlet length. Thus we are treating the fluid in the inlet length as if it were a pseudo-plastic non-Newtonian liquid. When a real pseudo-plastic non-Newtonian liquid is sheared, it is found that the apparent viscosity (as measured in a conventional viscosimeter) decreases as the rate of shear (or transverse velocity gradient dU/dr) increases. Thus:

$$\tau = \mu_{\text{apparant}} \left(\frac{dU}{dr}\right) = K \left(\frac{dU}{dr}\right)^n \tag{1}$$

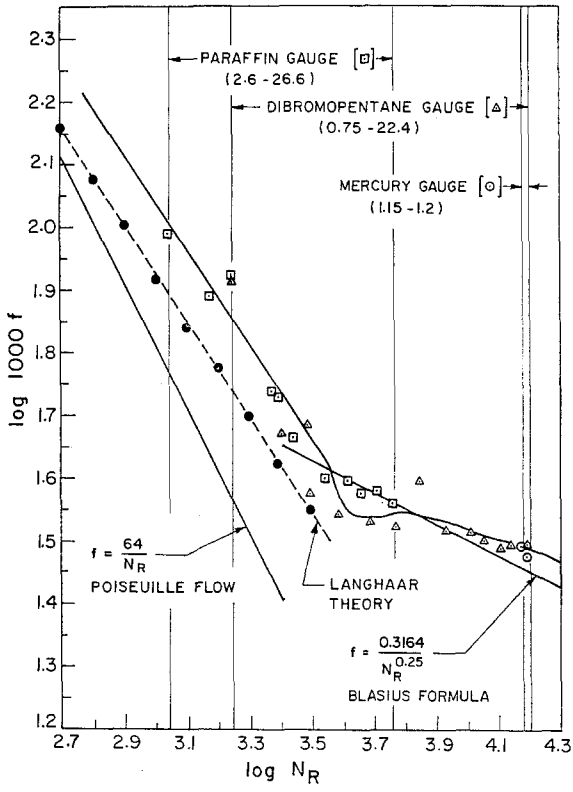

Figure 4. Test length 1–2: Variation of friction factor with Reynolds number at entry length of 16.5 diameters
(Figures in brackets indicate the range of the gauge reading in cm of liquid)

i.e.,

$$\mu_{\text{apparent}} = \frac{K}{\left(\frac{dU}{dr}\right)^{1-n}},$$

n being in fact < 1

Assuming pressure is a function of x only and is independent of r, then by applying the equilibrium of forces equation and integrating with the limits $U = 0$ at $r = r_0$ it can be easily shown that the velocity across the section and the friction factor due to the viscous forces are given by:

$$U = \left(\frac{-1}{2k}\frac{\partial P}{\partial x}\right)^{1/n}\left(\frac{n}{1+n}\right)\left(r_0^{\,n+1/n} - r^{n+1/n}\right) \tag{2}$$

and

$$f_v = 8\left(\frac{k}{\rho U_m D}\right)\left(\frac{D}{U_m}\right)^{1-n}\left(\frac{6n+2}{n}\right)^n \tag{3}$$

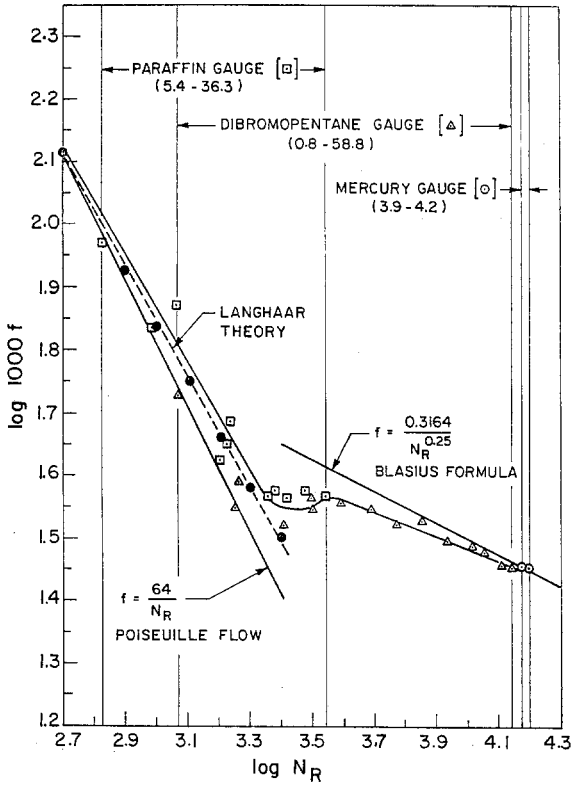

Figure 5. Test length 2–3: Variation of friction factor with Reynolds number at entry length of 51.4 diameters
(Figures in brackets indicate the range of the gauge reading in cm of liquid).

where U_m is the mean velocity $= Q/A$ and f_v is defined by Darcy's formula: $f_v = 2gDh/LU_m^2$

Relationship between 'n' *and the kinetic energy coefficient* 'α'

The limits of 'n' in the power law equation $\tau = K(\mathrm{d}U/\mathrm{d}r)^n$ are $n = 0$ when the velocity head correction factor $\alpha = 1$ (square velocity profile) and $n = 1$ when $\alpha = 2$ (parabolic velocity profile).

Consider equation (2): at $r = 0$, $U = U_c$ (i.e. maximum velocity at the centre of the pipe), and therefore U_c is given by:

$$U_c = \left(\frac{-1}{2K}\frac{\partial P}{\partial x}\right)^{1/n}\left(\frac{n}{1+n}\right)(r_0)^{(n+1)} \tag{4}$$

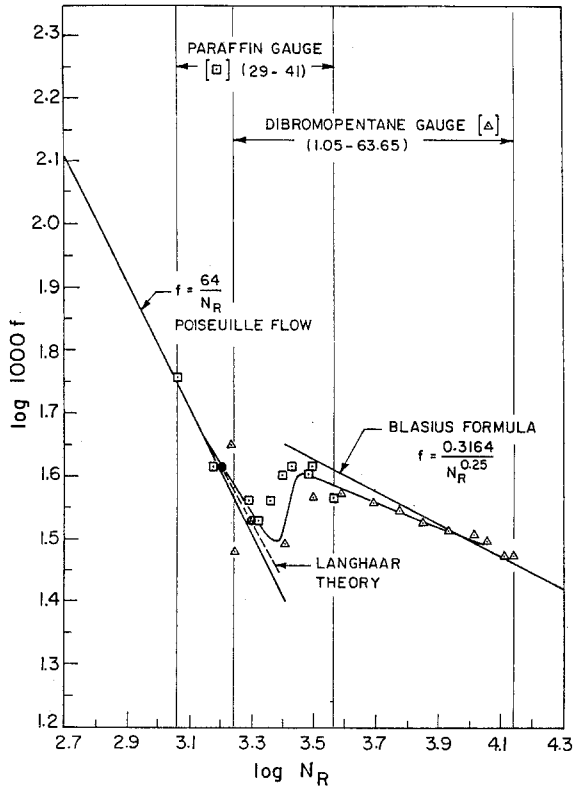

Figure 6.Test length 3–4: Variation of friction factor with Reynolds number at entry length of 106.9 diameters
(Figures in brackets indicate the range of the gauge reading in cm of liquid).

Dividing equation (2) by (4):

$$\frac{U}{U_c} = 1 - \left(\frac{r}{r_0}\right)^{n+1/n} \tag{5}$$

and similarly:

$$\frac{U}{U_m} = \left[\frac{3n+1}{1+n}\right]\left[1 - \left(\frac{r}{r_0}\right)^{n+1/n}\right]. \tag{6}$$

Using equation (5) to eliminate 'U' from equation (6):

$$U_c = U_m\left(\frac{3n+1}{1+n}\right) = \left(\frac{3n+1}{1+n}\right)\left(\frac{Q}{A}\right). \tag{7}$$

The kinetic energy (K.E.) = $\int_A U^2/2\ \mathrm{d}m$, where '$A$' is the area of the section

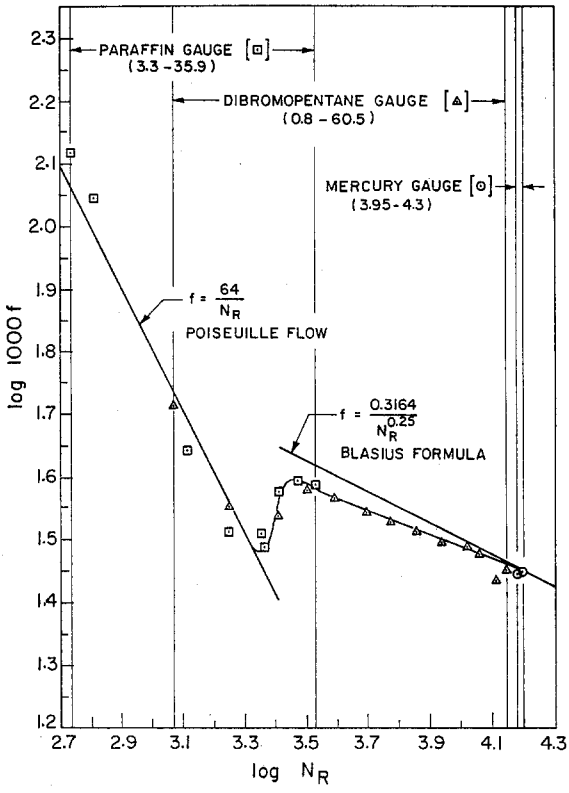

Figure 7. Test length 4–5: Variation of friction factor with Reynolds number at entry length of 163.2 diameters
(Figures in brackets indicate the range of the gauge reading in cm of liquid).

and 'm' is the total mass of fluid flowing across the section. '$\mathrm{d}m$' can be written in terms of $\mathrm{d}A$, δt, u and ρ. Hence the K.E. equation becomes:

$$\text{total K.E.} = \int_A \left(\frac{U^3}{2}\,\rho\,\partial t\right)\mathrm{d}A = \pi\,\rho\,\delta t \int^{r_0} U^3 r\,\mathrm{d}r$$

$$\text{K.E./sec} = \rho\,\pi \int^{r_0} U^3 r\,\mathrm{d}r.$$

Substituting for 'U' using equation (5) and evaluating the integrations:

$$\text{K.E./sec} = \frac{3\rho(3n+1)^2}{2(2n+1)(5n+3)}\left(\frac{Q^3}{A^2}\right)$$

but:

$$Q\rho = \text{mass/sec}$$

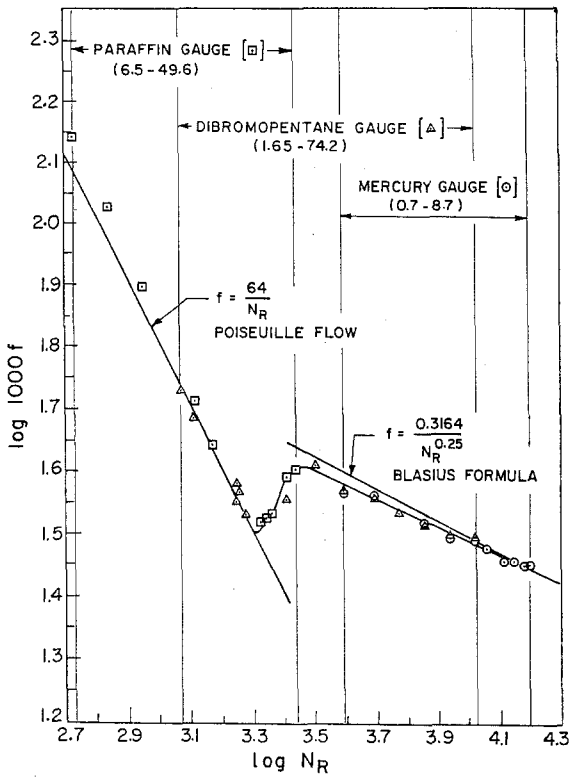

Figure 8. Test length 6–7: Variation of friction factor with Reynolds number at entry length of 361.7 diameters
(Figures in brackets indicate the range of the gauge reading in cm of liquid).

therefore

$$\text{K.E./mass} = \frac{3(3n+1)^2}{2(2n+1)(5n+3)}\left(\frac{Q^2}{A^2}\right)$$

$$\text{K.E./weight} = \frac{3(3n+1)^2}{2g(2n+1)(5n+3)}U_m^2. \tag{8}$$

Also:
$$\text{K.E./Weight} = \alpha\frac{U^2 m}{2g}. \tag{9}$$

Comparing equations (8) and (9):

$$\alpha = \frac{3(3n+1)^2}{(2n+1)(5n+3)}. \tag{10}$$

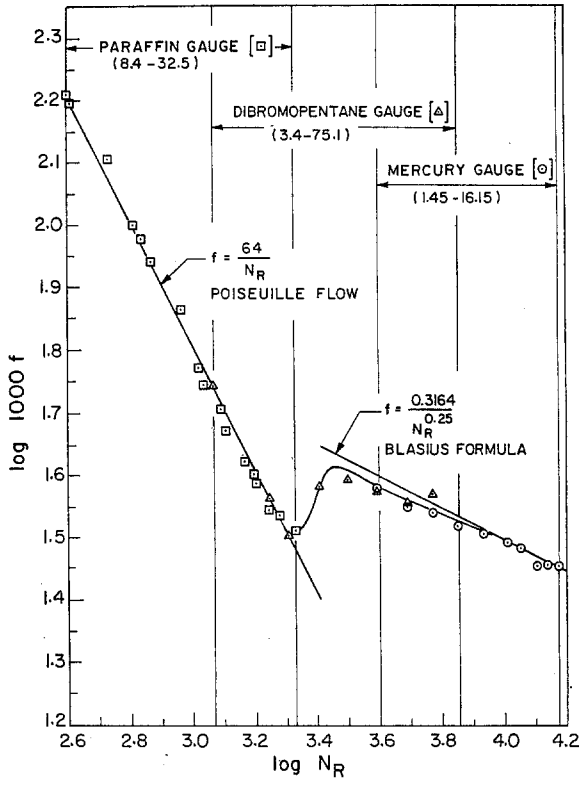

Figure 9. Test length 8–9: Variation of friction factor with Reynolds number at entry length of 756 diameters
(Figures in brackets indicate the range of the gauge reading in cm of liquid).

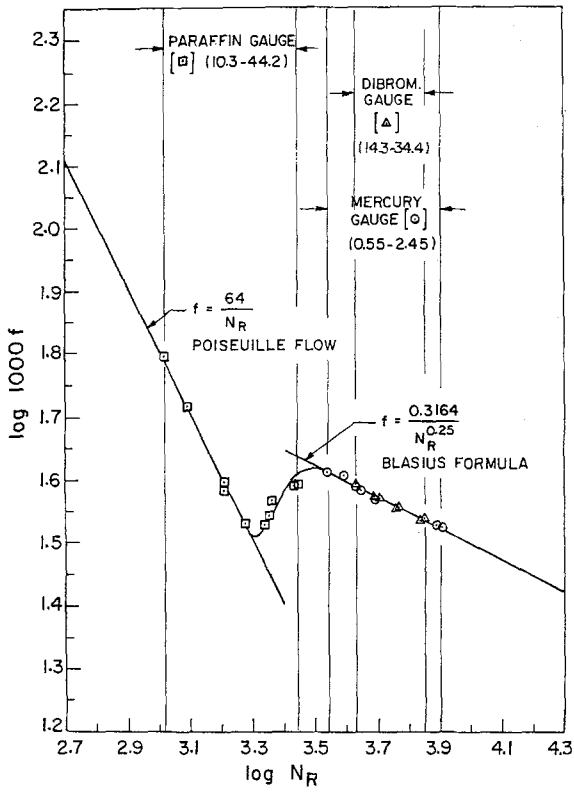

Figure 10. Test length 9–10: Variation of friction factor with Reynolds number at entry length of 919 diameters
(Figures in brackets indicate the range of the gauge reading in cm of liquid).

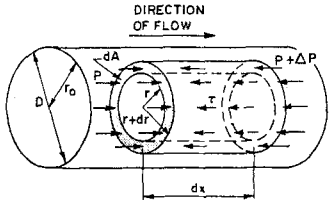

Figure 11. Study of flow in the inlet length.

Equation (10) is a useful relationship, and will be used in establishing an expression for f_k in terms of 'n' and N_R. A quick check can be made on the above relationship for $n = 0$ (square velocity profile) and $n = 1$ (parabolic velocity profile).

An expression for f_k

It is desirable now to derive a formula for evaluating the friction factor which is due only to the change in kinetic energy (velocity profile) in particularly the entry length and to the change in Reynolds number.

Consider the mass of fluid to be moving from section 1 to 2 over a distance ΔL, (Figure 12), where ΔL lies within the inlet length. The decrease in pressure energy per unit weight must equal the increase in kinetic energy per unit weight, i.e.:

$$\Delta\alpha \frac{U^2 m}{2g} = \frac{\Delta p}{\rho g}. \tag{11}$$

If we define f_k in the usual manner by:

$$\frac{\Delta p}{\rho g} = \frac{f_k U_m^2 \Delta L}{2gD} \quad \text{(Darcy's formula)}$$

then equation (11) becomes:

$$\Delta\alpha = f_k \frac{\Delta L}{D} = f_k \frac{\Delta L}{D} = f_k \frac{\Delta L}{2r} \tag{12}$$

Let:

$$Z = \frac{L}{r_0}$$

then:

$$\Delta Z = \frac{\Delta L}{r_0}.$$

Substituting for ΔL in equation (12) and re-arrangeing this equation:

$$f_k = 2\frac{\Delta\alpha}{\Delta Z} = 2\frac{d\alpha}{dZ}. \tag{13}$$

The above relationship is very simple and important, but it is desirable to write $d\alpha/dZ$ in terms of n, Z and N_R. Assuming that α is a function of n only (given by equation (10)), and n is a function of N_R and Z, then equation (13) can be written as:

$$f_k = 2\frac{d\alpha}{dZ} = \frac{d\alpha}{dn}\left[\frac{\partial n}{\partial Z}\right]_{N_R}. \tag{14}$$

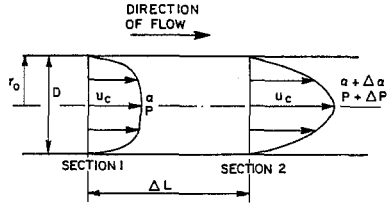

Figure 12. Velocity profile in the inlet length.

The term $d\alpha/dn$ in the above equation may be obtained by differentiating equation (10):

$$\frac{d\alpha}{dn} = \frac{117n^2 + 102n + 21}{(10n^2 + 11n + 3)^2} .$$

Therefore equation (14) becomes:

$$f_k = \frac{2(117n^2 + 102n + 21)}{(10n^2 + 11n + 3)^2} \left[\frac{\partial n}{\partial Z}\right]_{N_R} . \tag{15}$$

It can be seen from the above equation that in order to evaluate f_k we require a relationship between n, Z and N_R. Various researchers [4, 5, 11] constructed a family of curves for the velocity profile versus the entry length. From such curves we can develop the corresponding relationship between n, Z and N_R. The following theoretical relationship has been developed based on Langhaar's velocity profile results (Figure 13).

$$n = 751.5(\xi)^3 - 184.9(\xi)^2 + 19.97(\xi)$$

where

$$\xi = Z/N_R .$$

In Langhaar's results the fully developed parabolic profile is attained when $\xi = 0.114$, while in the present investigation the corresponding number is found to be 0.18 (Figure 14). Thus the above equation should be slightly adjusted to the following form:

$$n = 214.28(\xi)^3 - 102.52(\xi)^2 + 17.05(\xi). \tag{16}$$

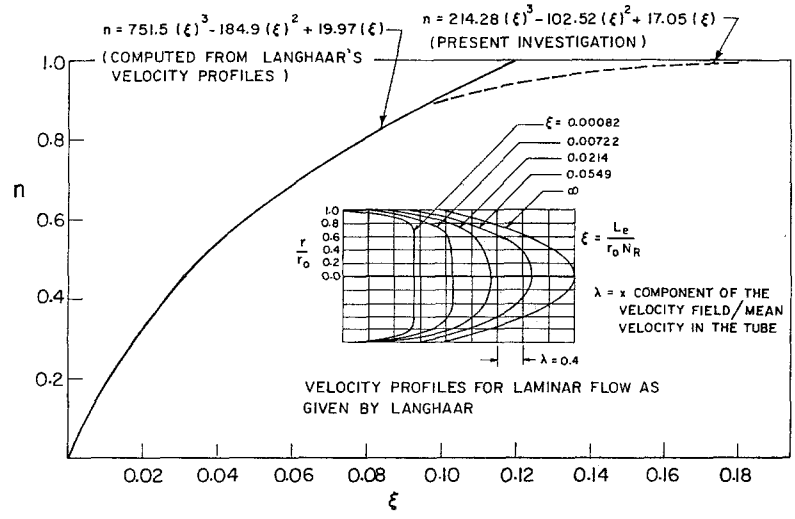

Figure 13. Variation of entry length/Reynolds number versus 'n'

Therefore:

$$\left[\frac{\partial n}{\partial Z}\right]_{N_R} = \frac{642.8}{N_R^3} Z^2 - \frac{205}{N_R^2} Z + \frac{17.05}{N_R}. \tag{17}$$

Thus, for a given N_R and Z, n and $\partial n/\partial Z$ may be determined using equations (16) and (17), and hence f_k is calculated from equation (15).

If the head loss over a length ΔL due to the viscous friction is ΔH_v and that due to the change in kinetic energy is ΔH_k, then in the present experiment the measured head loss is the total of the two and is equal to $\Delta H_v + \Delta_k H$. By considering the definitions of ΔH_v and ΔH_k in terms of the mean velocity U_m, it can easily be shown that the total friction factor f (measured) is given by:

$$f = f_v + f_k. \tag{18}$$

Variation of 'k' *with* 'n'

The preceding treatment of the Newtonian fluid in the inlet length as a pseudo-plastic non-Newtonian liquid resulted in an interesting attempt to establish a relationship between the viscous friction, the energy loss due the lengthwise rate of change of the kinetic energy coefficient and the total energy loss. Comparison of this imaginary behaviour with that of a real non-Newtonian liquid may be of interest at this stage.

It is known that the behaviour of many real non-Newtonian (or anomalous') liquids can be represented by equations of the form:

$$\tau = K\left(\frac{dU}{dr}\right)n$$

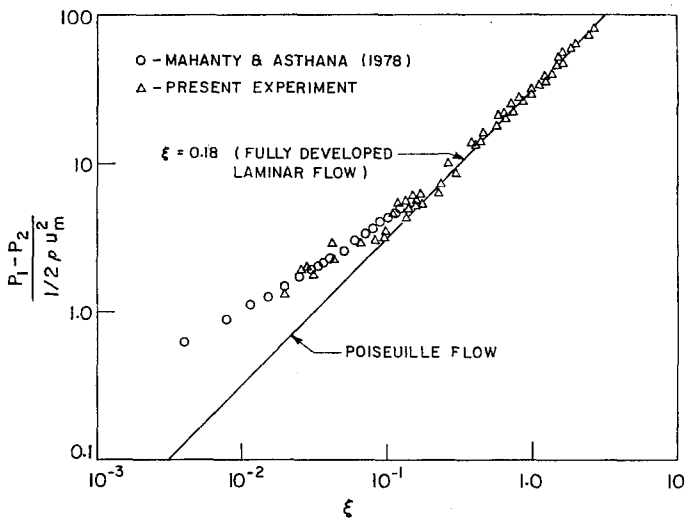

Figure 14. Dimensionless pressure drop versus entry length/Reynolds number

where K and n are sensibly constant (for a given liquid at a given temperature) over very large ranges of the rate of shear (dU/dr, sec^{-1}).

Now, when an anomalous liquid has its velocity estimated in a standard viscometer, the numerical value is naturally based on the Newtonian law $\tau = \mu(dU/dr)$, which we must now write as $\mu_{apparent}\,(dU/dr)$, since the value of μ will now be a function of (dU/dr). Hence, from the above equation:

$$\frac{K}{\mu_{apparent}} = \left(\frac{dU}{dr}\right)^{1-n}.$$

Consequently, K is the value of the apparent viscosity at unit rate of shear.

Experiments by Whittington [13] on aqueous solutions of the polymer methyl cellulose yield data (Table 2) from which the curves (at 1, 10 and 500 sec^{-1} shear rates) were plotted; (Figure 15). The apparent viscosity μ, and hence the ordinates K/μ for a genuine non-Newtonian liquid are obviously governed by the rate of shear, but for the fictitious non-newtonian water (during the lengthwise development of flow in the pipe), μ of course has a definite value, namely that of the viscosity of water. K/μ thus must become 1 as the flow develops into its final parabolic form, and n becomes 1. That is to say, K/μ proceeds from ∞ to 1 as n goes from 0 to 1.

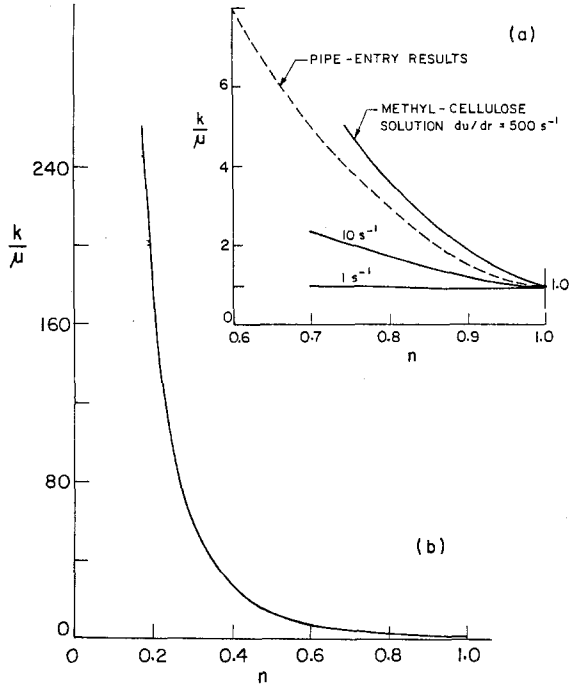

Figure 15. Variation of n with K/μ.

Table 2. Variation of 'K/μ' with 'n' at different rates of shear, for various pseudo-plastic liquids

The basic equation: $\log\frac{K}{\mu} = (1-n)\log\left(\frac{dU}{dr}\right)$; $\frac{K}{\mu} = 1$ when $\frac{dU}{dr} = 1\ \text{sec}^{-1}$

Liquid	Temp. (°C)	dU/dr (sec^{-1})	n	K	K/μ
Methyl-cellulose in water (2.52% cellulose)	20	10	0.742	5600	1.81
Methyl-cellulose in water (2.52% cellulose)	20	500	0.742	5600	4.97
Methyl-cellulose in water (1.88% cellulose)	20	10	0.848	3945	1.42
Methyl-cellulose in water (1.88% cellulose)	20	500	0.848	3945	2.57
Methyl-cellulose in water (1.39% cellulose)	20	10	0.906	1169	1.24
Methyl-cellulose in water (1.39% cellulose)	20	500	0.906	1169	1.80
Methyl-cellulose in water (1.24% cellulose)	20	10	0.944	238	1.14
Methyl-cellulose in water (1.24% cellulose)	20	500	0.944	238	1.42

Figure 15 (a and b) show the calculated variations of K/μ for the pipe-flow development, against a background of the genuinely shear-sensitive behaviour of the polymer solution, its viscosity falling dramatically as its molecules are orientated by rising values of the rate of shear.

The value of K/μ for the pipe-flow development are computed as follows: Consider equation (3) below:

$$f_v = 8\left(\frac{K}{\rho U_m D}\right)\left(\frac{D}{U_m}\right)^{1-n}\left(\frac{6n+2}{n}\right)^n . \tag{3}$$

If we define $N_R = U_m^D/\nu'$

then the above equation becomes:

$$K = \frac{f_v \rho (N_R \nu)^{2-n}}{8\left(\frac{6n+2}{n}\right)^n D^{2-2n}} . \tag{19}$$

Thus, for given values of N_R, n and f_v, the value of K can be obtained; ρ, D and ν are assumed to be constants.

Correlation between $f_v f_k$ and f

Figure 4 illustrated the variation of f with N_R for an entry length of 16.56 diameters, f being computed from the experimental measurements. For a given N_R the value of f_k, i.e. the component of the friction factor due to the

Table 3. Comparison between f_k, f_v and f_{exp} at an entry length of 16.5 diameters ($Z = 48$)

N_R	n	f_k (equations 15, 16 and 17)	f (present experiment)	$f_v = f - f_k$ (equation 18)	$64/N_R$
500	0.882	0.00631	0.18410	0.17779	0.12800
800	0.722	0.01051	0,12740	0.11689	0.08000
1000	0.606	0.01222	0.10720	0.09498	0.06400
1200	0.532	0.01307	0.09441	0.08134	0.05333
1400	0.473	0.01352	0.08222	0.06870	0.04571
1600	0.425	0.01372	0.07499	0.06127	0.04000
1800	0.386	0.01369	0.06761	0.05392	0.03556
2000	0.353	0.01349	0.06310	0.04961	0.03200
2200	0.325	0.01347	0.06138	0.04791	0.02909
2400	0.302	0.01314	0.05598	0.04284	0.02667
2500	0.290	0.01303	0.05433	0.04130	0.02560

change in velocity profile only, can be evaluated using the expression derived for f_k (equation 15) in conjunction with equations (16) and (17). f_v can be determined using the equation: $f_v = f - f_k$. This correlation may be tabulated in numerical form as shown in Table 3. Similar tables can be easily constructed for other entry lengths.

As can be seen from Figures 4–6, the shift from Poiseuille's fully developed flow in the $f - N_R$ curve based on Langhaar's theory is smaller than that given by the experimental results. Two reasons can be mentioned: (1) Given the state of development of the velocity profile, one can compute the 'f' arising from internal friction; but between any two pressure-tapping points the profile has changed, the kinetic-energy coefficient has changed, and there is a virtual f arising from this redistribution of velocity. (2) In Langhaar's theory, the velocity profile at a distance zero from the entrance is assumed to be uniform (i.e., $dU/dr = 0$); while in this investigation the entrance is sharp and the input velocity profile is not square even at low Reynolds numbers. Furthermore, it can be seen from Figures 4 and 5 that the shift between Langhaar's theory and the experimental results decreases as Reynolds number decreases, i.e. as the input velocity profile approaches a square shape.

Analysis and discussion of the results

The results of the experiments show that in the laminar region, and at a distance of fewer than 160 diameters from the entrance, the $f - N_R$ curve is shifted from the viscous law $f = 64/N_R$. The shift is higher near the entrance and rapidly decreases as the entrance is left behind. Also, for a particular test length, this shift is least at low Reynolds number and increases as Reynolds number increases. The equation of laminar flow, at a distance of 15 diameters from the entrance, is approximately $f = 21.4/N_R 0.8$ (Figure 4). This significant deviation from equation $f = 64/N_R$ is only found close to the entrance; so that over a distance of 100 diameters the flow equation coincides with the

$f = 64/N_R$ line up to a value of N_R of about 1400, and thereafter the deviation is very small (Figure 6). Moreover, at a distance of not more than 150 diameters from the entrance, the line $f = 64/N_R$ is completely obeyed (Figure 7).

In comparing the authors' experimental results with those of Langhaar's theory it should be recalled that Langhaar assumed an absolutely uniform velocity profile at the entry. In fact, the entry profile depends on the actual entrance shape as well as on the Reynolds number. One would therefore expect more deviation between the results of Langhaar and those of the authors near the entrance. The deviation between $N_R = 10^3$ and $N_R = 2 \times 10^3$ is about ± 5% in 'f' for an entry length of 16 diameters and is almost negligibly small for an entry length of approximately 51 diameters.

The results of Mohanty and Asthana [6] for the dimensionless pressure drop term $\{2(P_1 - P_2)/\rho U_m^2\}$ versus the entry length-Reynold's number $\{\xi\}$ was compared with those computed from the present experimental results as shown in Figure 14. The two results are very close and indicate that the Poiseuille flow is attained at ξ equalling approximately 0.16, which also agrees well with the measurements given by Fargie and Martin [3].

In conclusion, the postulation of an imaginary series of non-Newtonian liquids during the lengthwise development of a Newtonian fluid is an artifice yielding a simple, continuous change in the velocity distribution.

References

1. Campbell WD and Slattery JC (1963) Trans ASME (J Basic Eng). 85: 41.
2. Collins M and Schowalter JC (1963) AI Chem E J1 9: 804.
3. Fargie D and Martin B (1971) Proc Roy Soc A 321: 461.
4. Friedmann M, Gillis J. and Liron N (1968) Appl Sci Res 19: 426.
5. Langhaar HL (1942) Trans ASME (J Appl Mech) 9: 55.
6. Mohanty AK and Asthana SBL (1978) J Fluid Mech 90: 433.
7. Schiller L (1922) Z Agnew Math Mech 2: 96.
8. Schlichting H (1968) Boundary layer theory. McGraw-Hill.
9. Tatsumi T (1952) J Phys Soc Japan 7: 489.
10. Van Dyke MD (1970) J Fluid Mech 44: 813.
11. Vrentas JS and Duda JL (1973) Appl Sci Res 28: 241.
12. Whittington RB and Ashton EW (1948) M.Sc. thesis, Manchester University.
13. Whittington RB (1950) Internal report, St. Anthony Falls Hydraulic Laboratory, University of Minnesota, U.S.A.